



Timewise–dependent Coefficients Identification Problems for Third-Order Pseudo-Parabolic Equations from Nonlocal Extra Conditions

Sayl Gani^{1,2} , Mohammed S. Hussein^{3*}  Taysir E. Dyhoum⁴ 

¹Department of Mathematics, College of Education for Pure Sciences (Ibn AL-Haithem), University of Baghdad, Baghdad, Iraq.

²Department of Computer Techniques Engineering, Imam Al-Kadhun College, Baghdad, Iraq.

³Department of Mathematics, College of Science, University of Baghdad, Baghdad, Iraq.

⁴Department of Computing and Mathematics, Faculty of Science and Engineering, Manchester Metropolitan University, Manchester, UK.

*Corresponding Author.

Received:10 September 2023

Accepted:13 November 2023

Published:20 January 2025

doi.org/10.30526/38.1.3671

Abstract

This study aims to find the time-dependent potential terms in the two inverse problems of the third-order pseudo-parabolic with initial and various boundary conditions supplemented by the overdetermination data. The nonlinear inverse problems have significant applications in physics and engineering fields. We proved the existence and uniqueness of the solution of the two problems are being proved, but they still need to be proposed (since tiny perturbations in input data cause considerable errors in the output potential term). Consequently, the regularized methods should be employed. A finite difference schema is used for solving direct problems. In contrast, the inverse problems were reformulated as nonlinear least-square minimization and solved efficiently by optimizing MATLAB routine lsqnonlin. Tikhonov's regularization method was applied to get stable results. The numerical results were explained by presenting a test example for each problem. In addition, the stability was discussed by utilizing the Von Neumann stability analysis. The results showed that the time-dependent potential terms were reconstructed successfully and were stable and accurate.

Keywords: Von Neumann stability analysis, Finite difference method, Tikhonov regularization method, Pseudoparabolic inverse problem, Inverse problem.

1. Introduction

For the inverse problems, identifying the unknown coefficients of the parabolic problem has many applications in engineering and science. Many researchers have identified the unknown



coefficients of the parabolic inverse problem recently. For example, Hussian et al. investigated the parabolic inverse problem to identify the multiple time-dependent coefficients of thermal problems with unknown free boundary conditions in (1). Hussein and Lesnic investigated the one-dimensional parabolic inverse problem for determining the two time-dependent conductivity with Cauchy data and heat capacity storage in (2). While in (3), the authors presented two parabolic inverse problems for identifying the space and time-dependent coefficients from the overdetermination conditions. In (4), the authors presented the one-dimensional parabolic inverse problem for recovering the heat source and time-dependent thermal conductivity with the heat flux overdetermination condition for the other related work see (5-8).

The pseudo-parabolic equations of a higher order play an essential role in the mathematical modelling of moisture transfer, fluid filtration and heat propagation (9) and (10). The pseudo-parabolic inverse problems have been utilized in modelling various phenomena such as the wave processes, chemical, engineering, diffusion, plasma physics and heat conduction (11). In addition, they have many applications in real-life phenomena, such as the theory of small oscillation of a rotating fluid (12) and the infiltration of homogeneous fluids in strata (13). Moreover, Lyubonova and Tani (14) discussed the stabilization of a multi-dimensional pseudo-parabolic inverse problem with a coefficient of piezo conductivity and the regularity of the solution. In (15), the authors analyzed the uniqueness and existence of the solution of the third-order pseudo-parabolic inverse problem with periodic and integral conditions. Abylkairov and Khompysh (16) studied the existence and uniqueness of a solution for the right side of the pseudo-parabolic inverse problem, which was described as the motion of Kelvin - Voight fluids. Antotsev et al. (17) proved the unique solvability for the pseudo-parabolic inverse problem with a P-Laplacian and under a nonlocal integral overdetermination condition by using the Galerkin method. Many other researchers have examined the pseudo-parabolic inverse problem to identify the unknown time-dependent coefficients. In studies (18, 19), the pseudo-parabolic inverse problem was presented to determine the unknown coefficient of filtration and diffusion. In addition, the asymptotic behaviour of the pseudo-parabolic inverse problem to determine unknown source terms with integral conditions has been considered by Yaman and G'ozükizil (20).

A few years ago, the numerical solution containing unknown coefficients was investigated by Beshtokv for the pseudo-parabolic equations from a class of the third-order (21). The third-order pseudo-parabolic equations result from the problem with heat and moisture transmission and fluid filtration (22,23). An inverse problem of reformulating an unknown potential element has been studied (24). Moreover, both Huntual et al. (25,26) and Ramazanova et al. (27) examined the fourth-order inverse problem for identifying the time-dependent potential coefficient from additional conditions and the cubic-spline method as a direct method.

In this work, two pseudo-parabolic inverse problems were presented from the third-order equation to recover the potential time-dependent coefficient numerically with different boundary conditions. Since the periodic conditions were used for both problems, the Neuman and non-local integral conditions were used with the first and second problems, respectively. For both problems, the over-specification data was utilized for recovering the unique potential terms. The

uniqueness and existence were proved in (28) for the first problem and in (29) for the second one.

The formation of this study is as follows: Section 2 presents the mathematical form of the Inverse Problem I and II, which are contained in Subsection 1. The FDM is used to discretize the direct problems I and II, subsection 2, and the stability analysis is provided in subsection 3, Examples of tests for direct problems I and II. Section 3 presents the numerical technique of functional minimization and numerical results of the inverse problems I and II. Finally, in Section 4, the conclusions are highlighted.

2. Mathematical formulation of the inverse problem I and II

In rectangle domain $Q_T := \{0 \leq x \leq 1, 0 \leq t \leq T\}$, consider the inverse problems of identifying a pair of functions $(u(x, t), p(t))$, which satisfy the 1D pseudo-parabolic equation

$$\frac{\partial u(x, t)}{\partial t} = b \frac{\partial^3 u(x, t)}{\partial x^2 \partial t} + a(t) \frac{\partial^2 u(x, t)}{\partial x^2} + p(t) u(x, t) + f(x, t) \quad (x, t) \in Q_T \quad (1)$$

the initial condition

$$u(x, 0) = \varphi(x), \quad 0 \leq x \leq 1, \quad (2)$$

the periodic condition

$$u(0, t) = u(1, t), \quad 0 \leq t \leq T, \quad (3)$$

the Neumann condition

$$u_x(1, t) = 0, \quad 0 \leq t \leq T \quad (4)$$

the nonlocal integral condition

$$\int_0^1 u(x, t) dx = 0, \quad 0 \leq t \leq T \quad (5)$$

and the additional conditions are

$$u\left(\frac{1}{2}, t\right) + \int_0^1 u(x, t) dx = h_1(t), \quad 0 \leq t \leq T \quad (6)$$

$$u(x_0, t) = h_2(t), \quad 0 \leq t \leq T, \quad (7)$$

where $x_0 \in (0,1)$, and $b > 0$ is a given number.

We call Equations (1) - (4), (6) as the inverse problem I (IP-I) where a is constant and the Equations (1)-(3), (5), (7) as the inverse problem II (IP-II), where a is time-dependent function. In particular, if we put $b = 0$ in Equation (1), then the resulting is a heat equation which has been

investigated previously by many authors such as(7, 8, 30). The functions f, φ and h_1 and h_2 are given functions. In these problems, $p(t)$ is a potential term and (UX, t) is the temperature distribution, and these functions are unknown. These problems have been utilized in the modelling of various phenomena such as wave processes, chemical, engineering, diffusion, plasma physics and heat conduction (11). The unique solvability of IP-I has been established in (28), whilst for IP-II in (29) and the following their unique solvability theorems:

Definition: The classical solution of the IP-I and IP-II is the pair $\{u(x, t), p(t)\}$ satisfies the following properties:

- i- $u(x, t)$ is continuous in Q_T with all its derivatives.
- ii- $p(t)$ is continuous on $[0, T]$.
- iii- All Equation (1)– (5) conditions are satisfied in the ordinary sense.

Lemma 1 for IP-I: Suppose that $a > 0, b > 0, \varphi(x) \in C[0,1], f(x, t) \in C(Q_T), h_1(t) \in C^1[0, T], h_1(t) \neq 0$ for $(0 \leq t \leq T)$ and $\varphi\left(\frac{1}{2}\right) + \int_0^1 \varphi(x) dx = h_1(0)$. Then the problem of defining the functions $u(x, t)$ and $p(t)$ is equivalent to the problem of finding the solution of problem Equations (1)– (4), (6) possessing the properties (i) and (ii) of the solution of problem Equations (1)–(4), (6) from relations Equations (1)–(4), and

$$\begin{aligned} h_1'(t) + b \left(u_{tx}(0, t) + u_{txx}\left(\frac{1}{2}, t\right) \right) + a \left(u_x(0, t) + u_{xx}\left(\frac{1}{2}, t\right) \right) \\ = p(t)h_1(t) + f\left(\frac{1}{2}, t\right) \\ + \int_0^1 f(x, t) dx, \quad (0 \leq t \leq T) \end{aligned} \tag{8}$$

Theorem 1 for IP-I. Let the problem Equations (1) – (4), (8) satisfy the following conditions:

$$\begin{aligned} 1. \varphi(x) \in C^2[0,1], \quad \varphi'''(x) \in L_2(0,1), \\ \varphi(0) = \varphi(1), \quad \varphi'(1) = 0, \varphi''(0) \\ = \varphi''(1); \end{aligned} \tag{9}$$

$$\begin{aligned} 2. f(x, t) \in C(Q_T), \quad f_x(x, t) \in L_2(Q_T), \\ f(0, t) \\ = f(1, t), \quad (0 \leq t \\ \leq T). \end{aligned} \tag{10}$$

$$\begin{aligned} 3. a > 0, b > 0, \quad h_1(t) \in C^1[0, T], \quad h_1(t) \\ \neq 0 \quad (0 \leq t \\ \leq T). \end{aligned} \tag{11}$$

$$4. \varphi\left(\frac{1}{2}\right) + \int_0^1 \varphi(x) dx = h_1(0). \tag{12}$$

Then IP-I has a unique solution in the ball $K = K_R \|z\|_{E_T^3} \leq R = (A(T) + 2)$ of the space E_T^3 in Banach space.

where,

$$\begin{aligned} A(T) = & \frac{1}{3} \|\varphi(x)\|_{L_2(0,1)} + \frac{1}{3} \sqrt{T} \|f(x, t)\|_{L_2(Q_T)} \\ & + \|h_1^{-1}(t)\|_{C[0,T]} \left\| h_1'(t) - f\left(\frac{1}{2}, t\right) - \int_0^1 f(x, t) dx \right\|_{C[0,T]} \\ & + \left(\frac{\sqrt{6}}{2} + \frac{4a}{b^2} T + \frac{\sqrt{3a}}{3b} \|h_1^{-1}(t)\|_{C[0,T]} \right) \|\varphi'''(x)\|_{L_2[0,1]} \\ & + \left(\frac{\sqrt{6T}}{2b} + 4\left(\frac{1}{b} + \frac{a}{b^3} T\right) \sqrt{T} + \frac{\sqrt{3Ta}}{3b^2} \|h_1^{-1}(t)\|_{C[0,T]} \right) \times \|f_x(x, t)\|_{L_2(Q_T)} \\ & + 2\|x\varphi'''(x) + 3\varphi''(x)\|_{L_2(0,1)} + \frac{\sqrt{3}}{3} \|h_1^{-1}(t)\|_{C[0,T]} \\ & \times \|\|f_x(x, t)\|_{C[0,T]}\|_{L_2(0,1)}, \end{aligned} \tag{13}$$

$$\begin{aligned} B(T) = & \left(1 + \frac{1}{b} (2\sqrt{2} + \sqrt{3}) + \frac{4\sqrt{2}}{b} \left(1 + \frac{a}{b^2} T\right) \right) T \\ & + \left(\frac{a}{b} T + b\right) \|h_1^{-1}(t)\|_{C[0,T]}, \end{aligned} \tag{14}$$

Lemma 2 for IP-II: Suppose that $a(t) > 0$, $b > 0$, $a(t) \in C[0, T]$, $\varphi(x) \in [0, 1]$, $f(x, t) \in C(Q_T)$, $h_2(t) \in C^1[0, T]$, $h_2(t) \neq 0$, $\int_0^1 f(x, t) dx = 0$ for $(0 \leq t \leq T)$, $\int_0^1 \varphi(x) dx = 0$, $\varphi'(0) = \varphi'(1)$, $\varphi(x_0) = h_2(0)$. Then, the problem of defining the functions $u(x, t)$ and $p(t)$ is equivalent to the problem of finding the solution of IP-II, possessing the properties (i) and (ii) of the solution of IP-II, from relations (i)–(iii), and

$$\begin{aligned} u_x(0, t) = u_x(1, t), \quad & 0 \leq t \\ & \leq T, \end{aligned} \tag{15}$$

$$\begin{aligned} h_2'(t) - bu_{txx}(x_0, t) - a(t)u_{xx}(x_0, t) \\ = p(t)h_2(t) + f(x_0, t) \quad & (0 \leq t \leq T) \end{aligned} \tag{16}$$

Theorem 2 for IP-II. Let the problem Equations (1) – (3), (5), (16) satisfy the following:

1. $\varphi(x) \in C^2[0, 1]$, $\varphi'''(x) \in L_2(0, 1)$, $\varphi(0) = \varphi(1)$, $\varphi'(0) = \varphi'(1)$, $\varphi''(0) = \varphi''(1)$. (17)

$$2. \quad f(x, t) \in C(Q_T), \quad f_x(x, t) \in L_2(Q_T), \quad f(0, t) = f(1, t), \quad (0 \leq t \leq T). \quad (18)$$

$$3. a(t) > 0, b > 0, C [0, T], \quad h_2(t) \in C^1[0, T], \quad h_2(t) \neq 0 \quad (0 \leq t \leq T). \quad (19)$$

$$4. \varphi(x_0) = h_2(0). \quad (20)$$

Then IP- II has a unique solution in the ball $K = K_R \left(\|z\|_{E_T^3} \leq R = A(T) + 2 \right)$ of the space E_T^3 in Banach space.

Where

$$\begin{aligned} A_1(T) &= \|\varphi(x)\|_{L_2(0,1)} + \sqrt{T}\|f(x, t)\|_{L_2(Q_T)} + 2\sqrt{3}\|\varphi'''(x)\|_{L_2(0,1)} \\ &+ \frac{2\sqrt{3}}{b}\sqrt{T}\|f_x(x, t)\|_{L_2(Q_T)}, \end{aligned} \quad (21)$$

$$\begin{aligned} A_2(T) &= \|[h_2(t)]^{-1}\|_{C[0,T]} \left\{ \|h_2'(t) - f(x_0, t)\|_{C[0,T]} + \frac{2}{\sqrt{6}} \|f_x(x, t)\|_{C[0,T]} \|_{L_2(0,1)} \right. \\ &+ \frac{2}{\sqrt{6}} \|\varphi'(x)\|_{L_2(0,1)} \\ &+ \frac{2}{b\sqrt{6}} \|a(t)\|_{C[0,T]} (\|\varphi'(x)\|_{L_2(0,1)} \\ &\left. + \|f(x, t)\|_{L_2(Q_T)}) \right\} \end{aligned} \quad (22)$$

$$B_1(T) = \left(1 + \frac{2\sqrt{3}}{b} \right) T, \quad (23)$$

$$B_2(T) = \frac{2}{\sqrt{6}} \left(1 + \frac{1}{b^2} T \|a(t)\|_{C[0,T]} \right) \|[h_2(t)]^{-1}\|_{C[0,T]}, \quad (24)$$

where

$$A(T) = A_1(T) + A_2(T), \quad B(T) = B_1(T) + B_2(T). \quad (25)$$

2.1 Discretization of the direct solver

Consider the direct solver for IP-I contains the Equations (1)- (4) and required data Equation (6). Also, the direct solver for IP-II contains the Equations (1)-(3), (5) and the required data Equation (7). In these direct problems, the only unknown quantity that should be determined is

$u(x, t)$, that is, all other components are known. Discretising Equation (1) by a form of (FDM) as follows:

Denote for $u(x_i, t_j) = u_{i,j}$, and $f(x_i, t_j) = f_{i,j}$ where space node $x_i = i\Delta x$, time node $t_j = j\Delta t$, the space step length $\Delta x = \frac{1}{M}$ and time step length $\Delta t = \frac{T}{N}$ for $i = 0, 1, \dots, M$, $j = 0, 1, 2, \dots, N$ where M, N are positive integers. Based on the finite difference method, Equation (1) can be expressed as:

$$\frac{u_{i,j+1} - u_{i,j}}{\Delta t} = a_j \left(\frac{u_{i+1,j} - 2u_{i,j} + u_{i-1,j}}{(\Delta x)^2} \right) + \frac{b}{\Delta t} \left(\frac{u_{i+1,j+1} - 2u_{i,j+1} + u_{i-1,j+1}}{(\Delta x)^2} \right) - \frac{b}{\Delta t} \left(\frac{u_{i+1,j} - 2u_{i,j} + u_{i-1,j}}{(\Delta x)^2} \right) + p_j u_{i,j} + f_{i,j} \quad (26)$$

$$u(x, 0) = \varphi(x_i), \quad i = 0, 1, \dots, M, \quad (27)$$

$$u(0, t_j) = u(1, t_j), \quad j = 0, 1, \dots, N, \quad (28)$$

the Neumann condition

$$u_x(1, t) = 0 \text{ gives } u_{M+1,j} = u_{M-1,j}, \quad j = 0, 1, \dots, N \quad (29)$$

via central difference formula.

Using the trapezoidal rule approximation to the integral in Equation (5), we get the following formula

$$\sum_{i=1}^M u_{ij} = 0, \quad j = 0, 1, \dots, N. \quad (30)$$

Also, the approximate formula for overdetermination condition Equation (6) via trapezoidal rule is given as:

$$h_1(t_j) = u\left(\frac{M}{2}, t_j\right) + \frac{1}{M} \sum_{i=1}^M u_{ij}, \quad (31)$$

and the overdetermination condition Equation (7) is given as:

$$h_2(t_j) = u(x_0, j), \quad j = 0, 1, \dots, N. \quad (32)$$

Then, the discrete difference equation governing Equation (26) using the FDM scheme, we obtain the following difference equation.

$$-\alpha u_{i-1,j+1} + (1 + 2\alpha)u_{i,j+1} - \alpha u_{i+1,j+1} = \gamma_j u_{i-1,j} + (1 - 2\gamma_j + c_j)u_{i,j} + \gamma_j u_{i+1,j} + \Delta t f_{i,j}, \quad i = 1, 2, \dots, M, \quad j = 0, 1, 2, \dots, N, \quad (33)$$

where

$$\alpha = \frac{b}{(\Delta x)^2}, \quad \gamma_j = \frac{a_j \Delta t}{(\Delta x)^2} - \frac{b}{(\Delta x)^2}, \quad c_j = \Delta t p_j \quad (34)$$

The last difference Equation (33) can be encoded by the following linear system for Equations (1)-(4)

$$\mathbf{D}_1 v^{j+1} = \mathbf{E}_1 v^j + Z_1, \quad j = 0, 1, 2, \dots, N, \quad (35)$$

and for Equations (1)-(3) and (5)

$$\mathbf{D}_2 v^{j+1} = \mathbf{E}_2 v^j + Z_2, \quad j = 0, 1, 2, \dots, N, \quad (36)$$

where the matrices have the form

$$D_1 = \begin{pmatrix} 1 + 2\alpha & -\alpha & 0 & \dots & 0 & 0 & -\alpha \\ -\alpha & 1 + 2\alpha & -\alpha & \dots & 0 & 0 & 0 \\ \vdots & \vdots & \vdots & \ddots & \vdots & \vdots & \vdots \\ 0 & 0 & 0 & \dots & -\alpha & 1 + 2\alpha & -\alpha \\ 0 & 0 & 0 & \dots & 0 & -2\alpha & 1 + 2\alpha \end{pmatrix}_{M \times M}$$

$$D_2 = \begin{pmatrix} 2 & 2 & 2 & 2 & 2 & 2 & 0 \\ -\alpha & 1 + 2\alpha & -\alpha & 0 & 0 & 0 & 0 \\ 0 & -\alpha & 1 + 2\alpha & -\alpha & 0 & 0 & 0 \\ \vdots & \vdots & \vdots & \ddots & \vdots & \vdots & \vdots \\ 0 & 0 & 0 & \dots & -\alpha & 1 + 2\alpha & -\alpha \\ 0 & 2 & 2 & \dots & 2 & 2 & 2 \end{pmatrix}_{M+1 \times M+1}$$

$$E_1 = \begin{pmatrix} \gamma_j & 1 + 2\gamma_j + c_j & \gamma_j & 0 & \dots & 0 & 0 & 0 \\ 0 & \gamma_j & 1 + 2\gamma_j + c_j & \gamma_j & \dots & 0 & 0 & 0 \\ \vdots & \vdots & \vdots & \vdots & \ddots & \vdots & \vdots & \vdots \\ 0 & 0 & 0 & 0 & \dots & \gamma_j & 1 + 2\gamma_j + c_j & \gamma_j \\ 0 & 0 & 0 & 0 & \dots & 0 & 2\gamma_j & 1 + 2\gamma_j + c_j \end{pmatrix}_{M \times M}$$

$$E_2 = \begin{pmatrix} 0 & 0 & 0 & 0 & 0 & 0 & 0 \\ \gamma_j & 1 + 2\gamma_j + c_j & \gamma_j & 0 & 0 & 0 & 0 \\ 0 & \gamma_j & 1 + 2\gamma_j + c_j & \gamma_j & 0 & 0 & 0 \\ \vdots & \vdots & \vdots & \ddots & \vdots & \vdots & \vdots \\ 0 & 0 & 0 & \dots & \gamma_j & 1 + 2\gamma_j + c_j & \gamma_j \\ 0 & 0 & 0 & \dots & 0 & 0 & 0 \end{pmatrix}_{M+1 \times M+1}$$

$$Z_1 = \begin{pmatrix} \Delta t f_{1,j} \\ \Delta t f_{2,j} \\ \vdots \\ \Delta t f_{M-1,j} \\ \Delta t f_{M,j} \end{pmatrix}, \quad Z_2 = \begin{pmatrix} 0 \\ \Delta t f_{1,j} \\ \Delta t f_{2,j} \\ \vdots \\ \Delta t f_{M-1,j} \\ 0 \end{pmatrix},$$

where, $v^{j+1} = (u_{1,j+1}, u_{2,j+1}, \dots, u_{M,j+1})$ and $v^j = (u_{1,j}, u_{2,j}, \dots, u_{M,j})$.

2.2 Stability analysis

In this section, we apply the Von Neumann stability analysis (24, 31) for direct problems I and II. Assume that $f(x, t) = 0$, for simplicity, and local constant $p_j = \hat{g}$ for known time level in Equation (33) where $\hat{g} = \max_{t=[0,T]} |p(t)|$, and $\hat{a} = \max_{t=[0,T]} |a(t)|$, then we obtain:

$$-\alpha u_{i-1,j+1} + (1 + 2\alpha)u_{i,j+1} - \alpha u_{i+1,j+1} = \gamma u_{i-1,j} + (1 - 2\gamma + \Delta t * \hat{g})u_{i,j} + \gamma u_{i+1,j} \tag{37}$$

where,

$$\alpha = \frac{b}{(\Delta x)^2}, \quad \gamma = \frac{\hat{a}\Delta t}{(\Delta x)^2} - \frac{b}{(\Delta x)^2}, \tag{38}$$

Apply decomposition of the numerical solution into a Fourier sum as

$$u_{i,j} = S^j e^{wi\theta}, \tag{39}$$

where S is the amplification factor, the phase angle $\theta = \phi h$ where $\phi = \frac{2\pi}{N}$ and $w = \sqrt{-1}$. The amplification factor S is said to satisfy the von Neumann condition if $|S| < 1$. To find S, plug Equation (39) into Equation (37) as follows:

$$-\alpha S^{j+1} e^{w\theta(i-1)} + (1 + 2\alpha)S^{j+1} e^{wi\theta} - \alpha S^{j+1} e^{w\theta(i+1)} = \gamma S^j e^{w\theta(i-1)} + (1 - 2\gamma)S^j e^{w\theta(i)} + \gamma S^j e^{w\theta(i+1)}, \tag{40}$$

after simplifying above equation, we get:

$$-2\alpha S \left(\frac{e^{-w\theta} + e^{w\theta}}{2} \right) + (1 + 2\alpha)S = 2\gamma \left(\frac{e^{-w\theta} + e^{w\theta}}{2} \right) + (1 - 2\gamma), \tag{41}$$

This equation gives the following:

$$\begin{aligned} ((1 + 2\alpha) - 2\alpha \cos \theta)S \\ = (1 - 2\gamma) + 2\gamma \cos \theta \end{aligned} \tag{42}$$

Equation (42) which can be written as,

$$S = \frac{(1 - 2\gamma) + 2\gamma \cos \theta}{(1 + 2\alpha) - 2\alpha \cos \theta} \tag{43}$$

In order to ensure the stability, the last quantity should be less than one in the sense of absolute value, that is

$$\begin{aligned} |S| &= \left| \frac{(1 - 2\gamma) + 2\gamma \cos \theta}{(1 + 2\alpha) - 2\alpha \cos \theta} \right| \\ &< 1 \end{aligned} \tag{44}$$

This gives

$$\begin{aligned} |(1 + 2\alpha) - 2\alpha \cos \theta| &\leq |1 + 2\alpha| + 2\alpha |\cos \theta| \\ &\leq |1 + 2\alpha| \\ &+ 2\alpha, \end{aligned} \tag{45}$$

since $M > 0, \alpha = \frac{b}{(\Delta x)^2} = bM^2$, applying in Equation (45) this gives

$$\begin{aligned} \leq |1 + 2bM^2| + 2bM^2 &= 1 + 2bM^2 + bM^2 = 1 + 4bM^2 \\ &> 1 \end{aligned} \tag{46}$$

since $b > 0$ we guarantee that $|S| < 1$, therefor method is unconditionally stable.

The convergence of the proposed scheme is obtained from the Lax-Richtmyer equivalence theorem, which states that "a consistent finite-difference scheme for a linear non-fractional partial differential equation for which the initial-value problem is well posed is convergent if and only if it is stable". For a proof, see (32).

2.3 Examples of direct problems

2.3.1 Example for problem I

We consider the direct problem I Equations (1)-(4) with $T=1$ with $a = b = 0.01$ and the following input data:

$$\begin{aligned} u(x, 0) &= \frac{\cos(2\pi x)}{e^1}, \quad x \\ &\in [0,1] \end{aligned} \tag{47}$$

$$\begin{aligned} p(t) &= \cos(2\pi t), \quad t \\ &\in [0, T] \end{aligned} \tag{48}$$

$$f(x, t) = e^{-t}(-0.367879 - 0.367879 \cos(2\pi t)) \cos(2\pi x), \quad (x, t) \in Q_T \tag{49}$$

The analytic solution is given by

$$u(x, t) = e^{-1-t} \cos(2\pi x), \quad (x, t) \in Q_T, \tag{50}$$

and overdetermination condition

$$h_1(t) = -e^{-1-t}, \quad t \in [0, T]. \tag{51}$$

The numerical and exact solution of $u(x, t)$ and the absolute error is plotted in **Figure 1.** when $M = N = 40$. This figure shows the excellent matching with the error magnitude of order $O(10^{-3})$. **Figure 2.** presents the comparison between the exact solution and numerical for desired outputs $h_1(t)$. Also, excellent agreements were obtained.

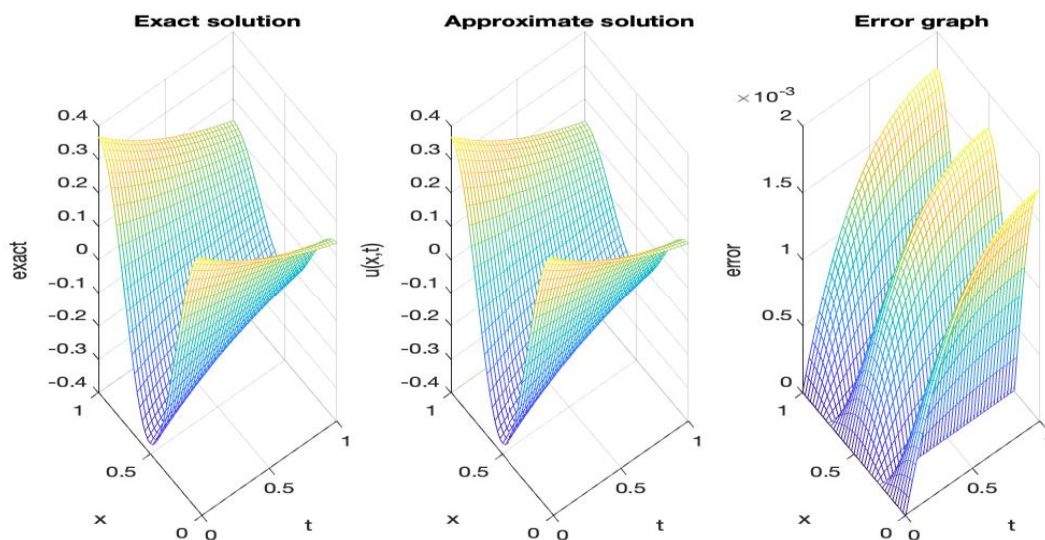


Figure 1. The exact and numerical solutions with an absolute error when $M = N = 40$, for Example, of the inverse problem I.

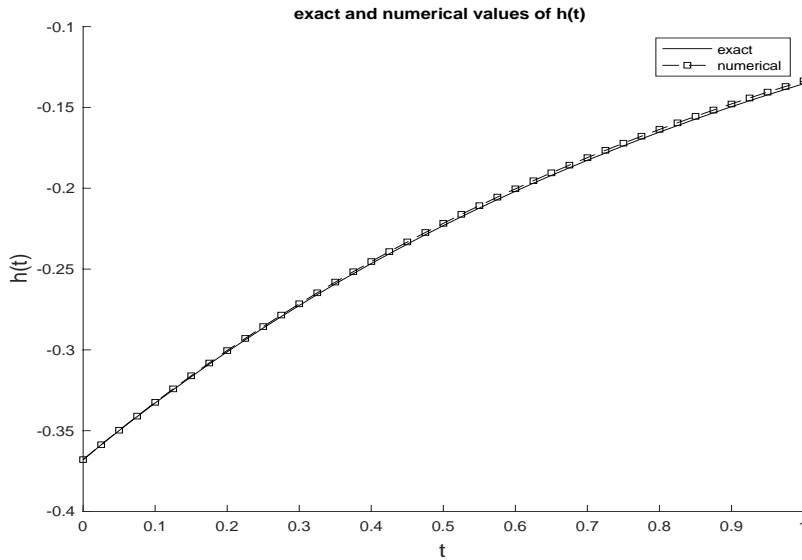


Figure 2. The required output $h_1(t)$, with $N = M = 40$, for Example of inverse problem I.

2.3.2 Example of Direct Problem II

Consider the direct problem II Equations (1)-(3) and (5) with $T=1$, $x_0 = \frac{1}{2}$, $a = b = 0.01$ and the following input data

$$u(x, 0) = -\frac{\cos(2\pi x)}{e^1}, \quad x \in [0,1], \tag{52}$$

$$p(t) = \sin(2\pi t), \quad t \in [0, T] \tag{53}$$

$$f(x, t) = \frac{1}{\sqrt{1+t}} e^{-\sqrt{1+t}} (0.697392 - 0.394784\sqrt{1+t}) + \sqrt{1+t} \sin(2\pi t) \cos(2\pi x), (x, t) \in Q_T \tag{54}$$

the analytic solution is given as

$$u(x, t) = -e^{-\sqrt{1+t}} \cos(2\pi x), \quad (x, t) \in Q_T \tag{55}$$

and overdetermination condition

$$h_2(t) = e^{-\sqrt{1+t}}, \quad t \in [0, T] \tag{56}$$

that can be checked by direct substitution.

Figure 3. presents the numerical solution, exact solution and the absolute error between them for the temperature $u(x, t)$ when $M = N = 40$. The figure shows an excellent agreement between

the exact and numerical solutions with the error magnitude of order $O(10^{-4})$. **Figure 4.** shows the comparison between the exact and numerical solutions of $h_2(t)$.

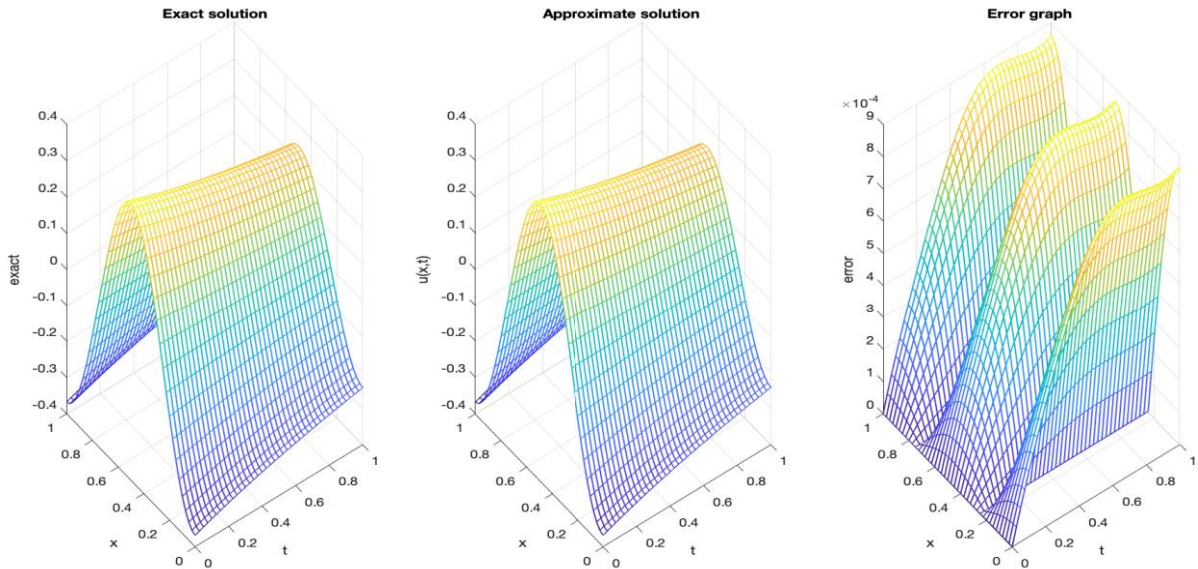


Figure 3. The exact and numerical solutions with the corresponding absolute error when $M = N = 40$, for Example, direct problem II.

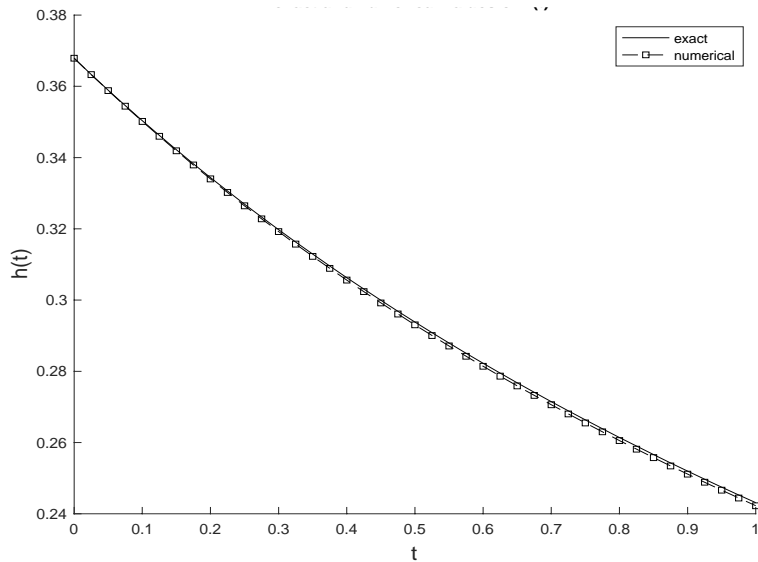


Figure 4. The required output $h_2(t)$, with $N = M = 40$, for Example of direct problem II.

3. Computational approach for inverse problems

Our goal in this section is devoted to solving IP-I and IP-II. To find stable reconstructions for unknown coefficient $p(t)$, in addition to heat distribution $u(x, t)$ which satisfy Equation (1)-(4), (6) for IP-I and Equations (1)-(3),(5), (7) for IP-II. These problems are reformulated as nonlinear

optimization problems and solved numerically by minimizing the gap between extra measurement data Equations (6) or (7) and the associated computed solution. To gain reliable results we apply the Tikhonov's regularization method due to the ill-posedness of the under investigation problems. The cost functional can be constructed as (33-40).

$$K_I(p) = \left\| \left[u\left(\frac{1}{2}, t\right) + \int_0^1 u(x, t) dx - h_1(t) \right] \right\|^2 + \beta \|p(t)\|^2, \quad (57)$$

for IP-I and the functional

$$K_{II}(p) = \|u(x_0, t) - h_2(t)\|^2 + \beta \|p(t)\|^2, \quad (58)$$

For IP-II, where $\beta \geq 0$ the regularization parameter, should be selected according to some selection strategy such as L-Curve (41), Mozorov disciperey principle (42), or trial and error as in (43, 44). The approximate form of the above functionals are:

$$K_I(\underline{p}) = \sum_{j=1}^N \left(u\left(\frac{1}{2}, t_j\right) + \int_0^1 u(x, t_j) dx - h_1(t_j) \right)^2 + \beta \sum_{j=1}^N p_j^2, \quad (59)$$

$$K_{II}(\underline{p}) = \sum_{j=1}^N \left(u(x_0, t_j) - h_2(t_j) \right)^2 + \beta \sum_{j=1}^N p_j^2, \quad (60)$$

For IP-I and IP-II, respectively.

The objective functions Equations (25) and (26), it is minimized via the subroutine *lsqnonlin* from the MATLAB optimization toolbox. This routine tries to solve nonlinear least-squares curve fitting problems starting from the initial guess for unknown coefficient p . The upper and lower bounds on the variable p are specified as $10^{-2} \leq p \leq 10^2$. Also, in this routine, there is no need to calculate the gradient separately; this is something impeded inside the routine package.

The following parameters are essential to initiate the optimization process of Equations (57) or (58); the minimization process will terminate when the following prescribed parameters are reached:

- Allowed number of iterations = 6000.
- Specified solution and objective function Tolerance = 10^{-20} .

The inverse problems I or II are solved concerning noisy/ exact measurement data in Equations (6) or (7). The additive noise type as presented in (45- 50):

$$h_l^\epsilon(t_j) = h_l(t_j) + \epsilon_j, \quad j = 1, 2, \dots, N, \quad l = 1, 2, \quad (61)$$

Where ϵ is a Gaussian random vector, and standard deviation μ is:

$$\mu_l = q \times \max_{t \in [0, T]} |h_l(t)|, \quad l = 1, 2, \quad (62)$$

Where q represents the percentage of noise. Here, we use the *normrnd* built-in function to generate the random variables $\epsilon = (\epsilon_j) \quad j = 1, 2, \dots, N$ as follows:

$$\epsilon = \text{normrnd}(0, \mu_l, N) \quad l = 1, 2 \quad (63)$$

3.1 Results and Discussion

We introduce a test example for each inverse problem. To explain the stability and accuracy of the computational procedure that is based on the finite difference method combined with the depreciation of Tikhonov's functional Equations (59) and (60).

To assess the reconstruction accuracy of the potential term, we use root mean squares error *rmse*, which is given by the following expression (51):

$$\begin{aligned} & rmse(p) \\ &= \sqrt{\frac{1}{N} \sum_{j=1}^N (p_j - p_{exact}(t_j))^2}, \end{aligned} \quad (64)$$

3.2 Numerical results for IP- I

Assume the inverse problem I with $T = 1$ and input data $a = b = 0.01$:

$$u(x, 0) = \frac{\cos(2\pi x)}{e^1}, \quad x \in [0, 1], \quad (65)$$

$$p(t) = \cos(2 \pi t), \quad t \in [0, T], \quad (66)$$

$$f(x, t) = e^{-t}(-0.367879 - 0.367879 \cos(2\pi t)) \cos(2\pi x), \quad (x, t) \in Q_T \tag{67}$$

with the analytic solution

$$u(x, t) = e^{-1-t} \cos(2\pi x), \quad (x, t) \in Q_T, \tag{68}$$

and overdetermination condition

$$h_1(t) = -e^{-1-t}, \quad t \in [0, T] \tag{69}$$

that can be checked by direct substitution.

Figure 5. shows the numerical solution of the time-dependent potential term from overdetermination Equation (6) in comparison with the exact solution ($p(t) = \cos(2\pi t)$), obtained by solving the IP-I with the above input data using the FDM, described in Section 2, with $M = N \in \{10, 20, 30, 40\}$. This figure shows that as mesh size increases, the retrieved coefficients converge to the exact solution, revealing that mesh independence occurs.

Figure 6. shows that the convergent objective function Equation (59) reaches a very low threshold stationary value of $O(10^{-8})$ and is plotted with $M = N \in \{10, 20, 30, 40\}$. From these figures, it can be observed a speed convergence is achieved in no more than 15 iterations only to reach a meagre value when $M = N = 40$, for example.

Next, we choose $N = M = 40$ for the rest of the numerical investigation, with cases ($q = 0\%, 0.5\%, 1\%$) included in the measurement data Equation (6). **Figure 7.** explains the plotting of the exact solution and numerical results for $p(t)$ with no regularization ($\beta = 0$) and no noise ($q = 0\%$) and noise $q \in \{0.5\%, 1\%\}$. It is clear that as the noise percentage increases from 0% to 1%, the identified coefficient has oscillatory behaviour, which is expected since the problem under investigation is ill-posed. Therefore, a sort of stabilization should be applied in order to restore stability and reduce the oscillatory behaviour.

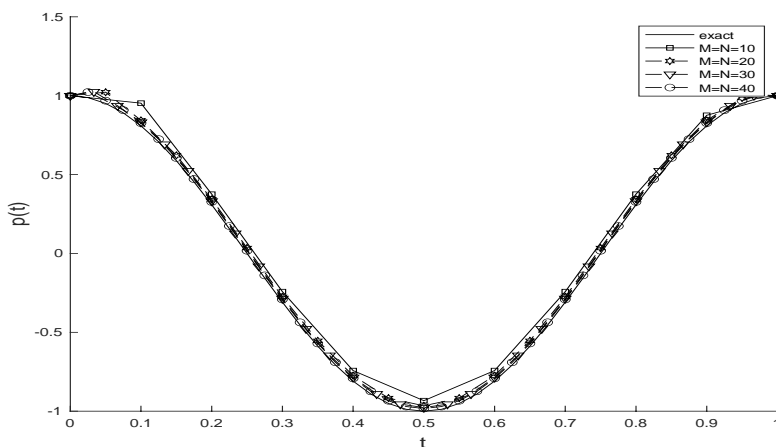


Figure 5. Numerical and exact solution for potential term $p(t)$ when $M = N \in \{10, 20, 30, 40\}$.

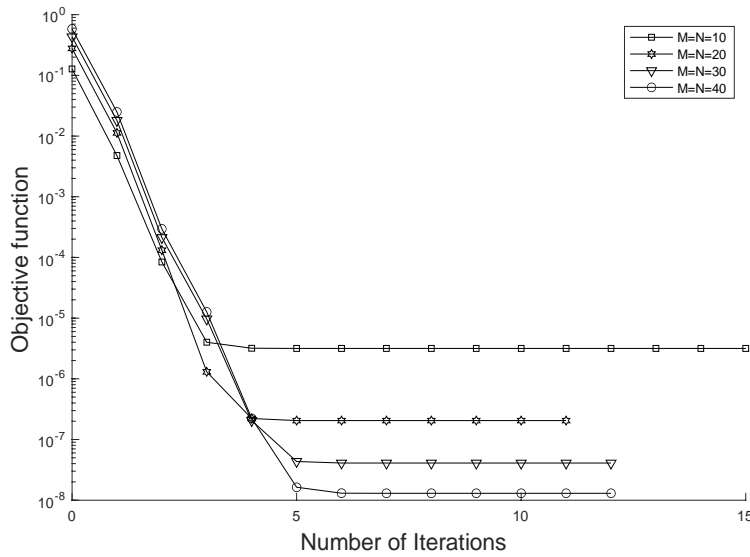


Figure 6. The unregularized objective function Equation (59), with $(q = 0)$ and $M = N \in \{10, 20, 30, 40\}$.

The associated numerical results for $p(t)$ after applying Tikhonov’s regularization method with $\beta \in \{10^{-4}, 10^{-5}, 10^{-6}\}$ for case $q = \{0.5\%\}$ and $\beta \in \{10^{-4}, 10^{-5}\}$ for case $q = \{1\%\}$ are presented in **Figures 8.** and **9.**, respectively. From this figure, one can deduce that as $\beta = 10^{-4}$ recover adequate identification with reasonable accuracy with $rmse(p) = \{0.2987, 0.3328\}$ for $q \in \{0.5, 1\}\%$ noise, respectively. The 3D graph for exact, numerical and absolute error between the exact solution and numerical solution for temperatures (UX, t) plotted in **Figure 10.** with **(a)** $q = 0.5\%$ and **(b)** $q = 1\%$ with $\beta = 10^{-4}$ and also accurate identification is obtained in terms of free oscillation. Next, in **Table 1.** we compute the $rmse$ values Equation (64) for $\beta \in \{10^{-i}, i = 4, 5, 6\}$ and $q \in \{0.5, 1\}\%$. **Figures 8, 9, 10.** and **Table 1.** show good correspondence and convergence between the numerical solutions of $p(t)$ and $u(x, t)$ with their corresponding exact solutions when q decreases from 1 % to 0.5% and then to 0%.

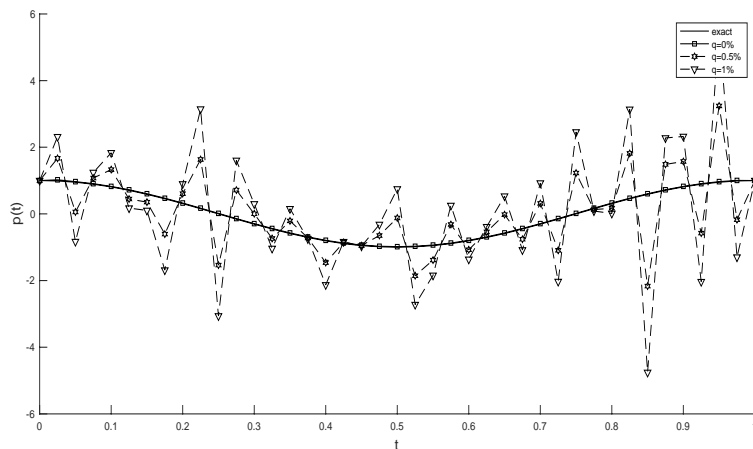


Figure 7. Numerical reconstructions and exact solution for $p(t)$, with noise level $q = \{0, 0.5\%, 1\%\}$, without regularization applied for IP- I.

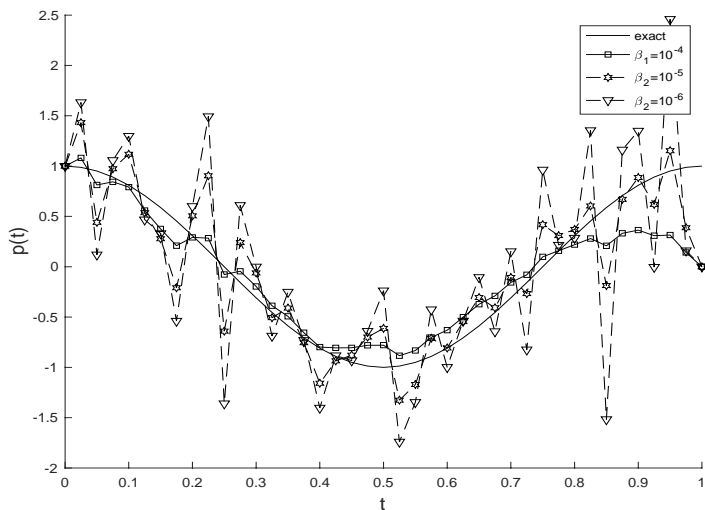


Figure 8. Numerical reconstructions and exact solution for $p(t)$, with regularization parameter $\beta = \{10^{-4}, 10^{-5}, 10^{-6}\}$ and $q = 0.5\%$ noise.

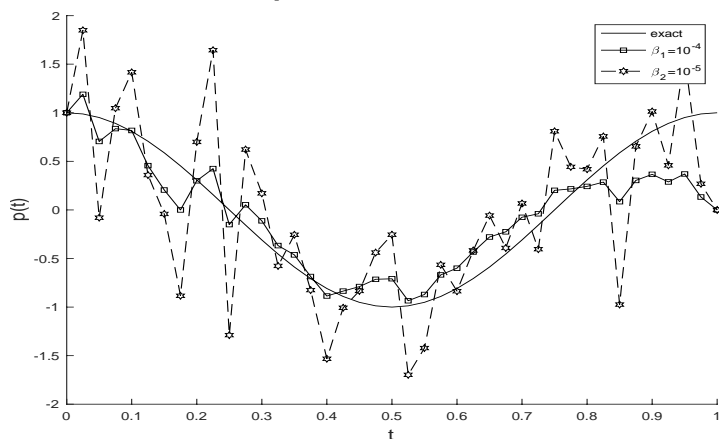
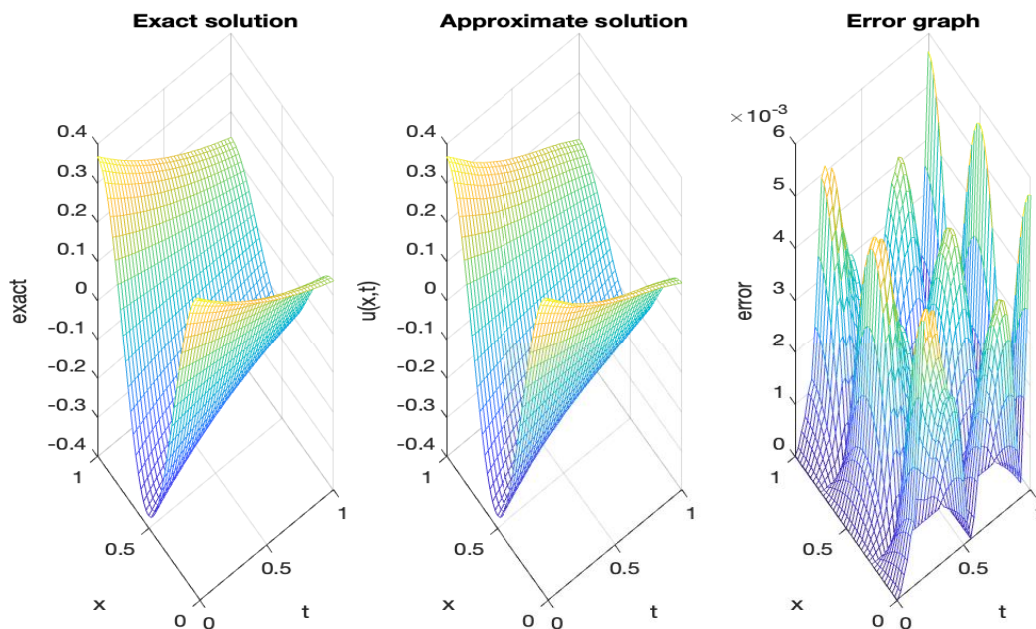
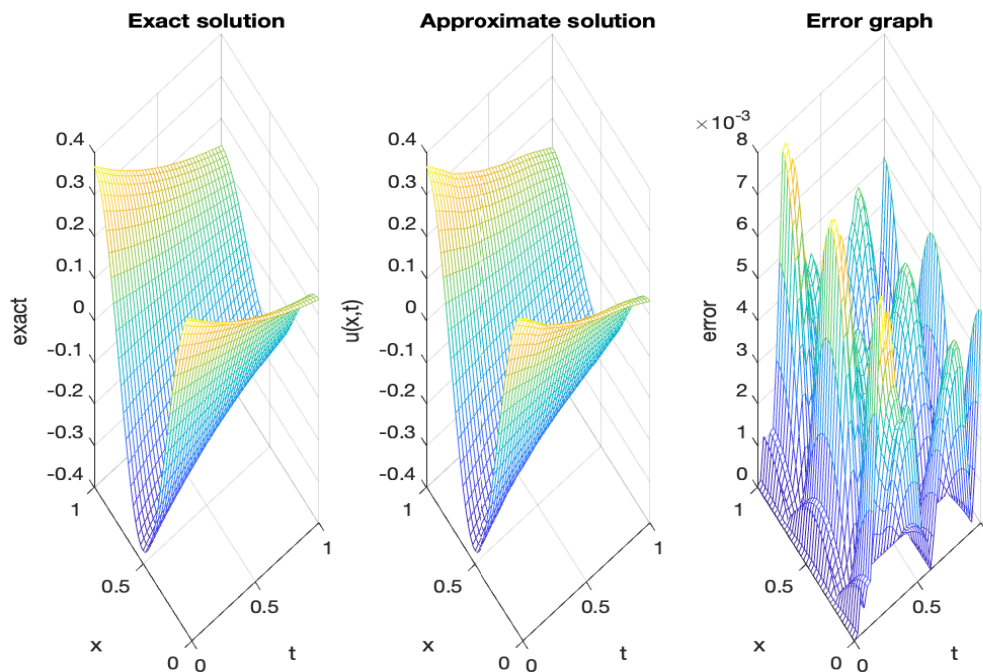


Figure 9. Numerical reconstructions and exact solution for $p(t)$, with regularization parameter $\beta = \{10^{-4}, 10^{-5}\}$ and $q = 1\%$ noise, for IP- I.



(a)



(b)

Figure 10. Numerical and exact temperature $u(x,t)$ with (a) $q = 0.5\%$ and $\beta = 10^{-4}$, (b) $q = 1\%$ noise and $\beta = 10^{-4}$, for IP-I.

Table 1. Numerical information for IP- I with various noise levels.

$q = 0.5\%$	$\beta = 10^{-4}$	$\beta = 10^{-5}$	$\beta = 10^{-6}$
No. of iterations	48	40	37
Objective function Equation (59) at the final iteration	0.0015	2.8078E-04	5.4229E-05
$rmse(p)$	0.2987	0.3678	0.7326
$q = 1\%$	$\beta = 10^{-4}$	$\beta = 10^{-5}$	$\beta = 10^{-6}$
No. of iterations	42	45	48
Objective function Equation (59) at the final iteration	0.0020	6.1036E-04	1.6380E-04
$rmse(p)$	0.3328	0.6661	1.4340

3.3 .Numerical results for IP- II

Consider the IP- II Equations (1)-(3),(5) and (7) with input data in Example 2.3.2. To solve this problem, we employ the same process presented in section 3.

Here, all the conditions of inverse problem II are satisfied, and hence, the unique solvability of the solution is guaranteed. Initially, we start with an initial guess when $t = 0$ (i. e $p(0) = 0$) and retrieve the function $p(t)$ and $u(x, t)$ for noise-free case ($q = 0$) (see **Figure 11.**), then for $q \in \{1\%, 3\%\}$ noisy data. From this figure, it is clear to observe the excellent matching when the mesh size is chosen as $M = N = 40$. the objective function Equation (60) is plotted as a function of the number of iterations in **Figure 12.** for noise-free cases and for noise included. The fast convergence can be seen to reach a very low value of $O(10^{-9})$ in just 11 iterations.

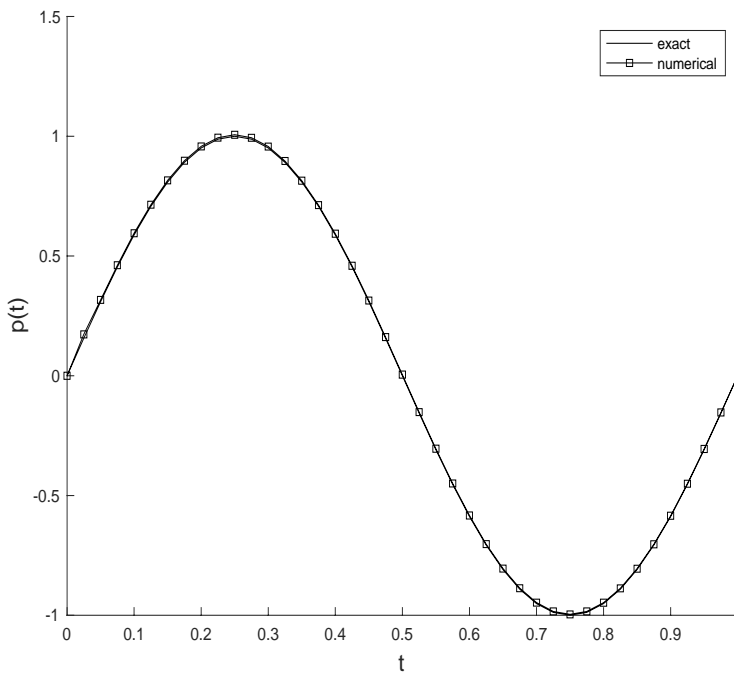


Figure 11. Numerical and exact solution for potential term $p(t)$ when $M = N = 40$, for Example, in IP-II.

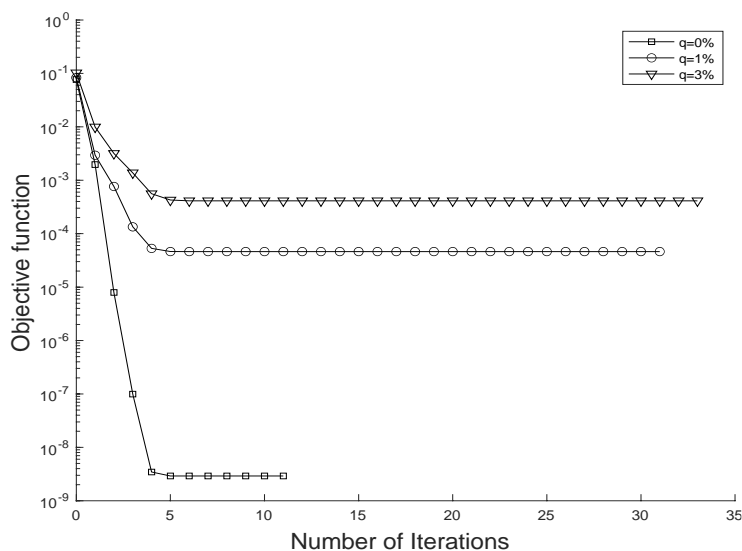


Figure 12. The unregularized objective function Equation (60), with $q = \{0, 1\%, 3\%$ noise data included in measurements Equation (7), for Example, in IP-II.

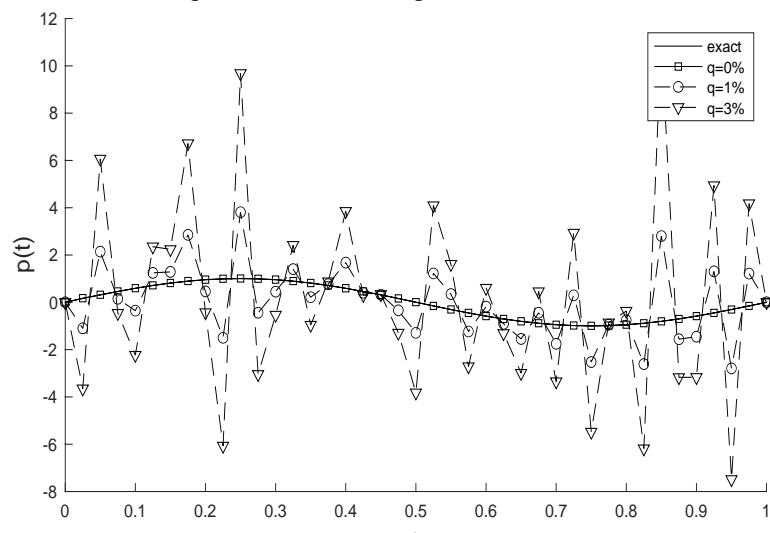


Figure 13. Numerical reconstructions and exact solution for $p(t)$, with noise level $q = \{0, 1\%, 3\%$, without regularization applied for IP- II.

For the cases plotted in **Figure 13.**, the results obtained were inaccurate and unstable when the regularization parameter was set $\beta = 0$ and $q \in \{1\%, 3\%\}$ —the Tikhonov regularization method employed to obtain stable reconstructions for $p(t)$. Regularization parameters $\beta = \{10^{-5}, 10^{-4}, 10^{-3}\}$ were chosen by trial and error strategy, which is based on starting from a small value for β and gradually increasing it until the oscillatory behaviour starts to disappear as applied in (40), for noise data $q = 1\%$. **Figure 15.** shows the objective function Equation (60) decreases steadily in just below 50 iterations. Tikhonov's approach with the selected parameters gives a reasonable and stable approximate solution of the potential term $p(t)$ (see **Figure 14.**). When $q = 3\%$, we deduce that the regularization parameters $\beta = \{10^{-4}$ and $10^{-3}\}$ give the stable and accurate approximate solution for $p(t)$ (see **Figures 16.** and **17.**). The 3D graphs of the exact and numerical solutions for $u(x, t)$, and the absolute error between are plotted in **Figure**

18. with (i) $q = 1\%$ and $\beta = 10^{-4}$, (ii) $q = 3\%$ and $\beta = 10^{-3}$. Other information about the number of iterations, the value of the objective function Equation (60) at the final iteration and the $rmse$ of $p(t)$ are given in **Table 2**. From **Figures 14, 16.** and **18.** and **Table 2.**, it can be seen that there is an adequate agreement between the numerical results of $p(t)$ and $u(x, t)$ for their analytical solutions.

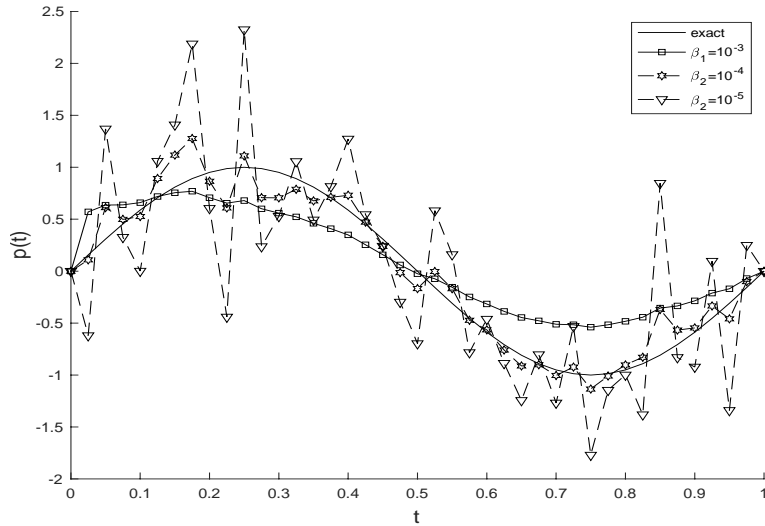


Figure 14. Numerical reconstructions and exact solution for $p(t)$, with regularization parameter $\beta = \{10^{-5}, 10^{-4}, 10^{-3}\}$ and $q = 1\%$ noise.

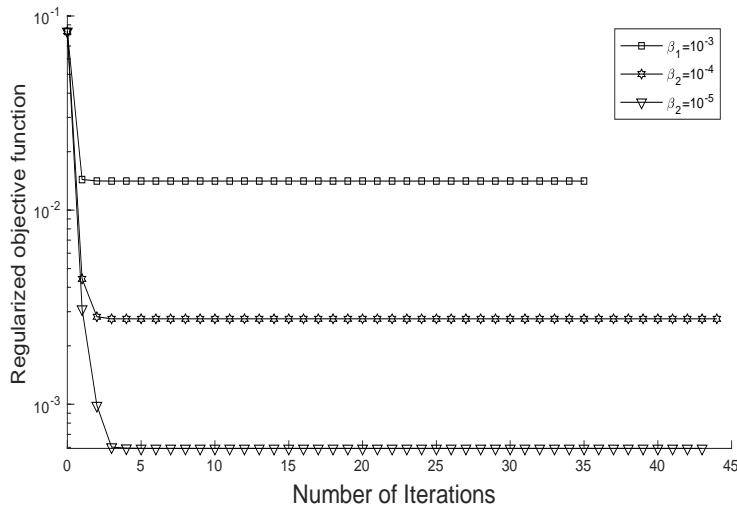


Figure 15. The regularized objective function Equation (60), with regularization parameter $\beta = \{10^{-5}, 10^{-4}, 10^{-3}\}$ and $q = 1\%$ noise.

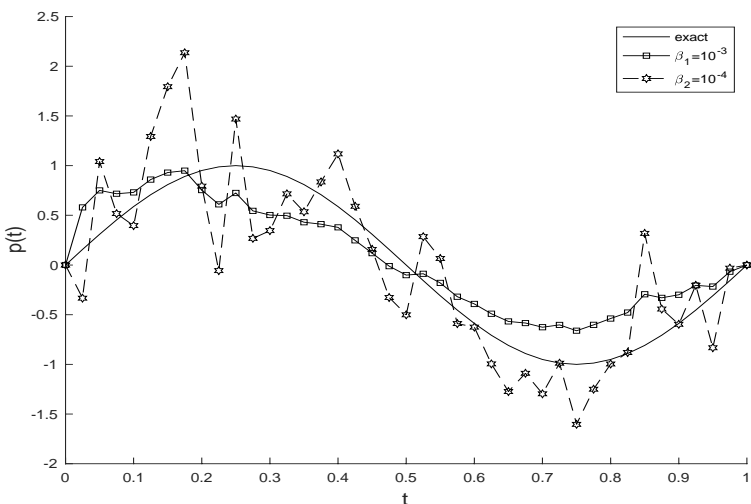


Figure 16. Numerical reconstructions and exact solution for $p(t)$, with regularization parameter $\beta = \{10^{-4}, 10^{-3}\}$ and $q = 3\%$ noise.

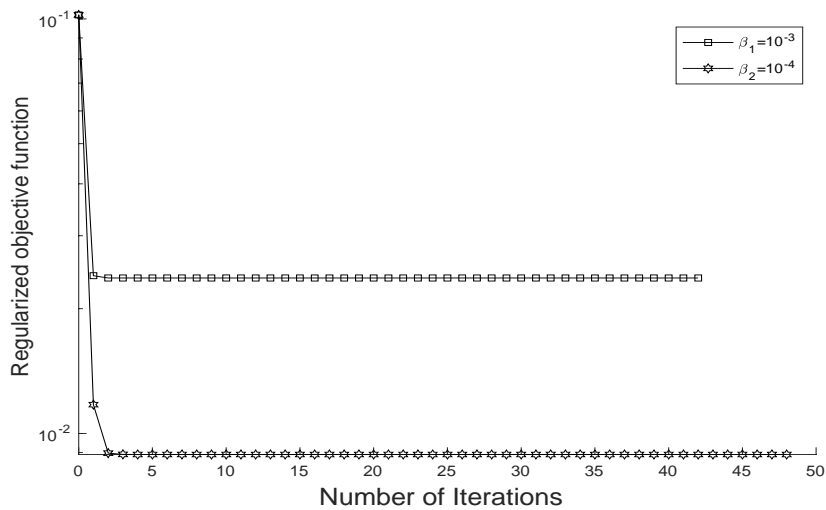


Figure 17. The regularized objective function Equation (60), with regularization parameter $\beta = \{10^{-4}, 10^{-3}\}$ and $q = 3\%$ noise.

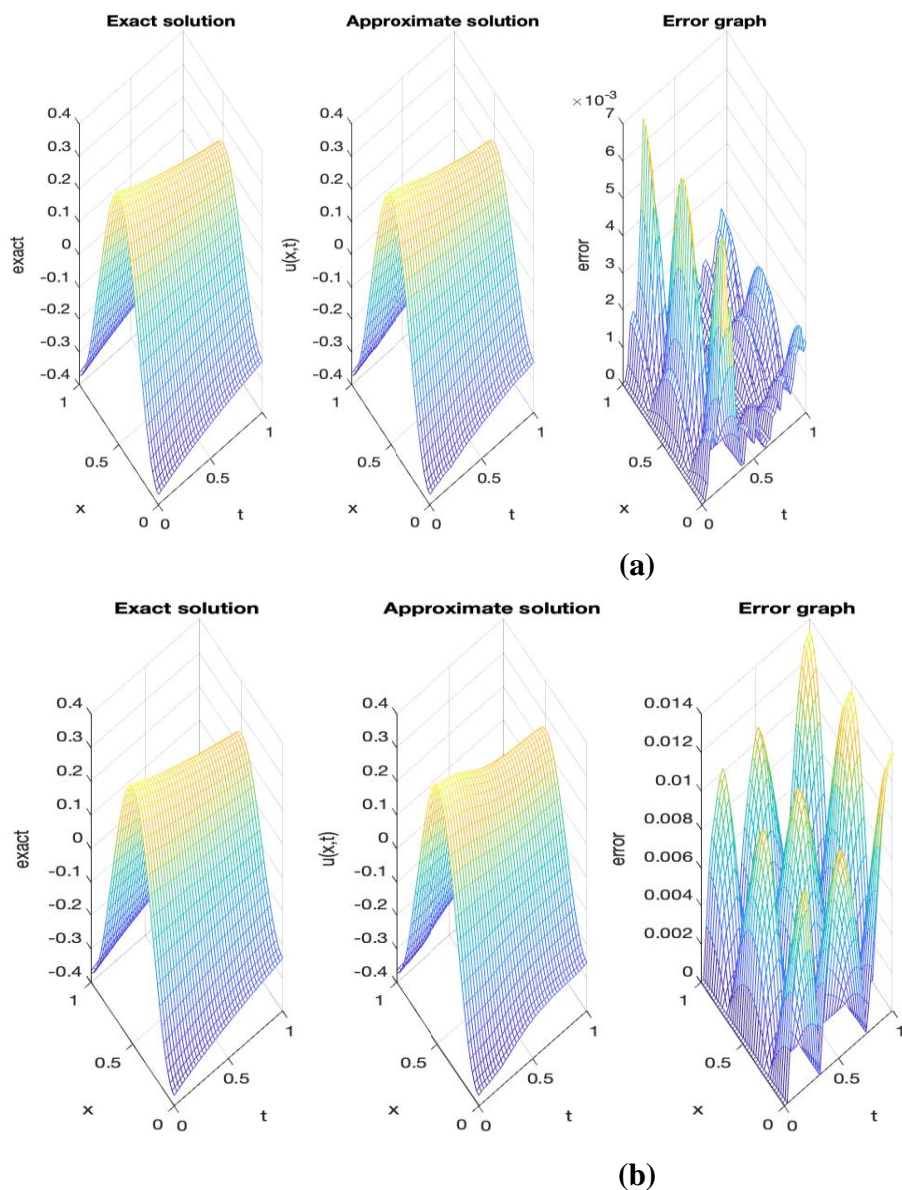


Figure 18. Exact and numerical temperature $u(x, t)$ with (a) $q = 1\%$ and $\beta = 10^{-4}$, (b) $q = 3\%$ noise and $\beta = 10^{-3}$.

Table 2. Numerical information for inverse problem II with noisy data and regularization.

	$q = 1\%$	$\beta = 10^{-3}$	$\beta = 10^{-4}$	$\beta = 10^{-5}$
No. of iterations		36	45	44
Objective function (60) at final iteration		0.0141	0.0028	5.9268E-04
$rmse(p)$		0.3054	0.1684	0.6502
	$q = 3\%$	$\beta = 10^{-3}$	$\beta = 10^{-4}$	$\beta = 10^{-5}$
No. of iterations		43	49	52
Objective function (60) at final iteration		0.0237	0.0089	0.0036
$rmse(p)$		0.2919	0.4942	1.9405

4. Conclusions

In this work, an investigation was conducted by considering the pseudo-parabolic equations of the third-order with initial and various boundary conditions and overdetermination data to

recover the time-dependent potential terms. The direct problems were solved by the FDM. Von Neumann technique was employed to study the stability of the proposed numerical direct algorithm. The inverse problems were reformulated as a nonlinear optimization problem and solved numerically by lsqnonlin iterative routine from MATLAB. To stabilize the ill-posed problem under investigation, Tikhonov's regularization method was applied. The numerical test examples for each problem confirmed the applicability of the proposed algorithm to obtain an accurate and stable solution. As a future work, it can apply this process to solve the other different inverse problems of higher dimensions.

Acknowledgements

We would like to express our gratitude other referees for their valuable comments and suggestions that led to a truly significant improvement of the paper.

Conflict of Interest

The authors declare that there are no competing interests regarding the publication of this paper.

Funding

This work is not supported by any the Foundation.

Ethical Clearance

Ethics of scientific research were carried out in accordance with international conditions.

References

1. Hussein M.S.; Lesnic D.; Ivanchov M.I.; SnitkoH A. Multiple time-dependent coefficient identification thermal problems with a free boundary. Applied numerical mathematics. 2016; 99: 24-50. <https://doi.org/10.1016/j.apnum.2015.09.001>
2. Hussein M.S.; Lesnic D. Identification of the time-dependent conductivity of an inhomogeneous diffusive material. Applied Mathematics and Computation. 2015; 269: 35-58. <https://doi.org/10.1016/j.amc.2015.07.039>
3. Hussein M. S.; Lesnic D. Simultaneous determination of time and space-dependent coefficients in a parabolic equation. Communications in Nonlinear Science and Numerical Simulation. 2016; 33: 194-217. <https://doi.org/10.1016/j.cnsns.2015.09.008>
4. Huntul M.J.; Hussein M. S. Simultaneous Identification of Thermal Conductivity and Heat Source in the Heat Equation. Iraqi Journal of Science. 2021; 1968-1978. DOI: 10.24996/ij.s.2021.62.6.22
5. Hazanee A.; Lesnic D.; Ismailov M.I.; Kerimov N. B. Inverse time-dependent source problems for the heat equation with nonlocal boundary conditions. Applied Mathematics and Computation. 2019; 346, 800-815. <https://doi.org/10.1016/j.amc.2018.10.059>
6. Hussein M.S.; Adil Z. Numerical solution for two-sided Stefan problem. Iraqi Journal of Science. 2020; 61.2: 444-452. <https://doi.org/10.24996/ij.s.2020.61.2.24>
7. Hazanee A.; Lesnic D. Reconstruction of multiplicative space-and time-dependent sources. Inverse Problems in Science and Engineering. 2016; 24(9), 1528-1549. <https://doi.org/10.1080/17415977.2015.1130041>
8. Qassim M.; Hussein M.S. Numerical Solution to Recover Time-dependent Coefficient and Free

- Boundary from Nonlocal and Stefan Type Overdetermination Conditions in Heat Equation. Iraqi Journal of Science. 2021; 950-960. <https://doi.org/10.24996/ijs.2021.62.3.25>
9. Asanov A.; Atamanov E.; Nonclassical and inverse problems for pseudo-parabolic equations, 1997, Vol. 7. VSP.
 10. Colton D. Pseudoparabolic equations in one space variable. Journal of Differential Equations. 1972; 12(3):559–565. <https://core.ac.uk/reader/82773480>
 11. Khompysh, K. Inverse problem for 1D pseudo-parabolic equation, Springer New York LLC. 2017; 216, 382–387. <https://doi.org/10.100>
 12. Sobolev, S. L. On a new problem of mathematical physics. In Selected Works of S.L. Sobolev. 2006; 279–332. Springer. <https://doi.org/10.1007/978-0-387-34149-1>
 13. Barenblatt G.I.; Zheltov I. P.; Kochina I. N. Basic concepts in the theory of seepage of homogeneous liquids in fissured rocks [strata]. Journal of applied mathematics and mechanics. 1960; 24 (5):1286–1303.
[https://blasingame.engr.tamu.edu/z_zCourse_Archive/P620_14C/P620_14C_zReference/\(Barenblatt_Zheltov_Kochina\)_Basic_Concepts_in_the_Theory_of_Seepage_of_Homogeneous_Liquids_in_Fissured_Rocks.pdf](https://blasingame.engr.tamu.edu/z_zCourse_Archive/P620_14C/P620_14C_zReference/(Barenblatt_Zheltov_Kochina)_Basic_Concepts_in_the_Theory_of_Seepage_of_Homogeneous_Liquids_in_Fissured_Rocks.pdf)
 14. Lyubanova A.S. and Tani A. An inverse problem for the pseudo-parabolic equation of filtration: the stabilization. *Applicable Analysis*. 2013; 92(3):573–585. <https://doi.org/10.1080/00036811.2011.630667>
 15. Mehraliyev Y. T.; Shafiyeva G.K. Inverse boundary value problem for the pseudoparabolic equation of the third order with periodic and integral conditions. *Applied Mathematical Sciences*. 2014; 8(23):1145–1155. <http://dx.doi.org/10.12988/ams.2014.4167>
 16. Abylkairov U. U.; Khompysh K. H. An inverse problem of identifying the coefficient in kelvin-voight equations. *Appl Math Sci*. 2015; 9(101-104):5079–5088. <http://dx.doi.org/10.12988/ams.2015.57464>
 17. Antontsev S. N.; Aitzhanov S. E.; Ashurova G. R. An inverse problem for the pseudo-parabolic equation with p-laplacian. *Evolution Equations and Control Theory*. 2022; 11(2):399. <http://dx.doi.org/10.3934/eect.2021005>
 18. Lyubanova A. S. Inverse problem for a pseudoparabolic equation with integral overdetermination conditions. *Differential Equations*. 2014; 50.4: 502-512. <https://doi.org/10.1134/S0012266114040089>
 19. Lyubanova A. Sh.; and Tani A. An inverse problem for the pseudo-parabolic equation of filtration: the existence, uniqueness and regularity. *Applicable Analysis*. 2011; 90.10: 1557-1571. <https://doi.org/10.1080/00036811.2010.530258>
 20. Yaman M.; Özukizil G.; Faruk Ö. Asymptotic behaviour of the solutions of inverse problems for pseudo-parabolic equations. *Applied mathematics and computation*. 2004; 154.1: 69-74. [https://doi.org/10.1016/S0096-3003\(03\)00691-X](https://doi.org/10.1016/S0096-3003(03)00691-X)
 21. Barenblatt G. I.; Zheltov Y. P.; Kochina I. N. Basic concept in the theory of seepage of homogeneous liquids in fissured rocks. *J. Appl. Math. Mech*. 1960; 24, 1286–1303.
[https://blasingame.engr.tamu.edu/z_zCourse_Archive/P620_14C/P620_14C_zReference/\(Barenblatt_Zheltov_Kochina\)_Basic_Concepts_in_the_Theory_of_Seepage_of_Homogeneous_Liquids_in_Fissured_Rocks.pdf](https://blasingame.engr.tamu.edu/z_zCourse_Archive/P620_14C/P620_14C_zReference/(Barenblatt_Zheltov_Kochina)_Basic_Concepts_in_the_Theory_of_Seepage_of_Homogeneous_Liquids_in_Fissured_Rocks.pdf)
 22. Rubinshtein L. I. On heat propagation in heterogeneous media. *Izvestiya Rossiiskoi Akademii Nauk. Seriya geograficheskaya*. 1948; 12, 27–45.
 23. Ting T.W. A cooling process according to the two-temperature theory of heat conduction. *J. Math. Anal. Appl*. 1974; 45, 23–31. [https://doi.org/10.1016/0022-247X\(74\)90116-4](https://doi.org/10.1016/0022-247X(74)90116-4)

24. Huntul M. J.; Dhiman N.; Tamsir, M. Reconstructing an unknown potential term in the third-order pseudo-parabolic problem. *Comput. Appl. Math.* 2021; 40: 140.
25. Huntul M. J.; Tamsir M.; Dhiman N. An inverse problem of identifying the time dependent potential in a fourth-order pseudo-parabolic equation from additional condition. *Num. Meth. Part. Differential Equations.* 2021. <https://doi.org/10.1002/num.22778>.
26. Huntul M. J. Determination of a time-dependent potential in the higher-order pseudo-hyperbolic problem. *Inverse Prob. Sci. Eng.* 2021. <https://doi.org/10.1080/17415977.2021.1964496>.
27. Ramazanov A. T.; Mehraliyev Y. T.; Allahverdieva S. I. On an inverse boundary value problem with non-local integral terms condition for the pseudo-parabolic equation of the fourth order. *Differential equations and their applications in mathematical modelling.* 2019; 101–103. <https://conf.svmo.ru/files/2019/papers/paper32>.
28. Mehraliyev Y.; Shafiyeva T.; Gulshan Kh. Determination of an unknown coefficient in the third-order pseudo-parabolic equation with non-self-adjoint boundary conditions. *Journal of Applied Mathematics.* 2014. <https://doi.org/10.1155/2014/358696>
29. Mehraliyev Y. T.; Shafiyeva G. Inverse boundary value problem for the pseudo-parabolic equation of the third order with periodic and integral conditions. *Applied Mathematical Sciences.* 2014; 8(23), 1145-1155. <http://dx.doi.org/10.12988/ams.2014.4167>
30. Dhiman N.; Tamsir, M. A collocation technique based on a modified form of trigonometric cubic b-spline basis functions for Fisher's reaction-diffusion equation. *Multidiscipline Modeling in Materials and Structures.* 2018; 14:923–939, 10. <https://doi.org/10.1108/MMMS-12-2017-0150>
31. Sousa E. On the edge of stability analysis. *Applied Numerical Mathematics.* 2009; 59(6): 1322-1336. <https://doi.org/10.1016/j.apnum.2008.08.001>
32. Strikwerda J. C. *Finite Difference Schemes and Partial Differential Equations.* Pacific Grove, CA: Wadsworth and Brooks, 1989.
33. Alosaimi M.; Lesnic D.; Niesen J. Identification of the thermo-physical properties of a stratified tissue. Adiabatic hypodermic wall. *International Communications in Heat and Mass Transfer.* 2021; 126, 105376. <https://doi.org/10.1016/j.icheatmasstransfer.2021.105376>
34. Cao Kai.; Lesnic D.; Ismailov M. I. Determination of the time-dependent thermal grooving coefficient. *Journal of Applied Mathematics and Computing.* 2021; 65: 199-221. <https://doi.org/10.1007/s12190-020-01388-7>
35. Hussein M. S.; Lesnic D.; Kamynin V. L.; Kostin, A. B. Direct and inverse source problems for degenerate parabolic equations. *Journal of Inverse and Ill-Posed Problems.* 2020; 28.3: 425-448. <https://doi.org/10.1515/jiip-2019-0046>
36. Alosaimi M.; Lesnic D.; B. T. Johansson B. T. Solution of the Cauchy problem for the wave equation using iterative regularization. *Inverse Problems in Science and Engineering.* 2021;29(13): 2757-2771. <https://doi.org/10.1080/17415977.2021.1949590>
1. 37. Anwer F.; Hussein M. S. Retrieval of timewise coefficients in the heat equation from nonlocal overdetermination conditions. *Iraqi Journal of Science.* 2022; 1184–1199. <https://doi.org/10.24996/ij.s.2022.63.3.24>
37. Hussein M. S.; Lesnic D.; Johansson B. T.; Hazanee A. A. Identification of a multidimensional space-dependent heat source from boundary data. *Applied Mathematical Modelling.* 2018; 54:202–220. <https://doi.org/10.1016/j.apm.2017.09.029>
38. Hussein M. S.; Kinash N. S. E. P.; Lesnic D.; Ivanchov, M. Retrieving the time-dependent thermal conductivity of an orthotropic rectangular conductor. *Applicable Analysis.* 2017; 96.15: 2604-2618. <https://doi.org/10.1080/00036811.2016.1232401>

39. Ibraheem Q. W.; Hussein M. S. Determination of time-dependent coefficient in time-fractional heat equation. *Partial Differential Equations in Applied Mathematics*. 2023; 100492. <https://doi.org/10.1016/j.padiff.2023.100492>
40. Hansen, P. C. Analysis of discrete ill-posed problems by means of the l-curve. *SIAM review*. 1992; 34(4):561–580. <https://doi.org/10.1137/1034115>
41. Morozov V. A. On the solution of functional equations by the method of regularization. In *Doklady Akademii Nauk. Russian Academy of Sciences*. 1966; 167: 510–512. <http://www.mathnet.ru/eng/agreement>
42. Hussein S. O. Determination force/source function dependent on space under the non-classical condition data. *Journal of University of Babylon for Pure and Applied Sciences*. 2020; 28(3): 68-75. <https://www.journalofbabylon.com/index.php/JUBPAS/article/view/3333/2546>
43. Hussein S. O. Splitting the one-dimensional wave equation. Part I: Solving by finite-difference method and separation variables. *Baghdad Science Journal*. 2020; 17(2 (SI)): 0675-0675. [http://dx.doi.org/10.21123/bsj.2020.17.2\(SI\).0675](http://dx.doi.org/10.21123/bsj.2020.17.2(SI).0675)
44. Alosaimi M. A.; Lesnic D. Determination of the space-dependent blood perfusion coefficient in the thermal-wave model of bio-heat transfer. *Engineering Computations*. 2023; 129: 34-49. <https://doi.org/10.1108/EC-07-2022-0467>
45. Alosaimi M.; Lesnic D. Determination of a space-dependent source in the thermal-wave model of bio-heat transfer. *Computers & Mathematics with Applications*. 2023; 129: 34-49. <https://doi.org/10.1016/j.camwa.2022.10.026>
46. Hussein S. O, Placement Inverse Source Problem under Partition Hyperbolic Equation. *Iraqi Journal of Science*. 2021; 1994-1999. <https://doi.org/10.24996/ijs.2021.62.6.25>
47. Hussein S. O; T. E. Dyhoum. Solutions for non-homogeneous wave equations subject to unusual and Neumann boundary conditions. *Applied Mathematics and Computation*. 2022; 430, 127285. <https://doi.org/10.1016/j.amc.2022.127285>
48. Karami A.; Abbasbandy S.; Shivanian E. Inverse problem of identifying a time-dependent coefficient and free boundary in heat conduction equation by using the meshless local Petrov-Galerkin (MLPG) method via moving least squares approximation. *Filomat*. 2020; 34(10): 3319-3337. <https://doi.org/10.2298/FIL2010319K>
49. Karami A.; Abbasbandy S.; Shivanian E. Meshless local Petrov–Galerkin formulation of inverse Stefan problem via moving least squares approximation. *Mathematical and Computational Applications*. 2019; 24(4): 101. <https://doi.org/10.3390/mca24040101>
50. Huntul M. J.; Tamsir M. Reconstruction of a potential coefficient in the Rayleigh–Love equation with non-classical boundary condition. *Engineering Computations*. 2022; 39(10): 3442-3458. <https://doi.org/10.1108/EC-01-2022-0010>